C. R. Physique 3 (2002) 1293–1303

Physique appliquée/*Applied physics*

DOSSIER

MÉCANISMES PHYSIQUES DU NUAGE D'ORAGE ET DE L'ÉCLAIR
THE PHYSICS OF THUNDERCLOUD AND LIGHTNING DISCHARGE

A new model of charge transfer during ice–ice collisions

Marcia Baker [a], Jon Nelson [b]

[a] **Depts of Earth and Space Science and Atmospheric Sciences, University of Washington, Seattle, WA 98195-1310, USA**

[b] **Nelson Scientific, 7-13-8 Oginosato Higashi Otsu, Shiga 520-0248, Japan**

Note presented by Guy Laval.

Abstract We present a new model of charge transfer between two particles of ice that collide and then rebound. We calculate the charge distribution near the surface of an ice particle both in equilibrium and during growth or sublimation. Using simplified but plausible geometrical descriptions of the colliding surfaces we calculate the mass that is melted by the excess pressure at the point of contact, and we assume that electric charge is transferred from the sharper to the flatter particle with the melted material. Our predictions are in semiquantitative agreement with charge transfer measurements from several laboratories. ***To cite this article: M. Baker, J. Nelson, C. R. Physique 3 (2002) 1293–1303.***

electrification / thunderstorms / ice surface / charge transfer

Un nouveau modèle décrivant le transfert de charge lors d'une collision entre particules de glace

Résumé Nous présentons un model décrivant l'échange de charge électrique entre deux particules de glace qui entrent en collision et se séparent. Nous calculons la distribution de charge près de la surface d'une particule de glace, soit en état d'équilibre, soit pendant la croissance ou sublimation. Sur la base de considérations géométriques simples mais plausibles, nous calculons la masse d'eau fondue sous l'effet de la pression au point de contact, et nous supposons que le transfert de charge électrique associé s'effectue à partir de la particule à plus faible rayon de courbure. Les predictions du modèle sont globalement en accord avec les observations de plusieurs laboratoires. ***Pour citer cet article : M. Baker, J. Nelson, C. R. Physique 3 (2002) 1293–1303.***

électrisation / orages / surface de glace / transfert de charge électrique

E-mail address: baker@ess.washington.edu (M. Baker).

S1631-0705(02)01408-1/FLA

1. Introduction

The initial buildup of thundercloud electric fields has been the study of many laboratory and theoretical studies, which are excellently reviewed by [1–3]. These studies have shown that microphysical processes are responsible for the early accumulation of nonuniform electric charge distributions inside clouds. The prime mechanism for creation of these charge distributions appears to be collisions between rimed and unrimed ice particles that result in net charge accumulation on each of the collision partners. The sign and magnitude of the transferred charge depend on many parameters; at $T \leqslant -10$ °C in strong updrafts, corresponding to the conditions within which most of the relevant collisions occur in thunderclouds, the collisions leave the heavier (rimed), downward moving particles predominantly negatively charged, whereas the lighter, vapor grown particles become positively charged and move upward. At higher temperatures and high EW the rimed particles may become positively charged as they fall. Thus an electric dipole or possibly tripole can be formed which can produce enormous electric fields on the order of 10^5 V·m^{-1}. The mechanism of charge transfer during collisions of previously uncharged ice particles is as yet not well understood, and forms the subject of this paper.

1.1. Review of laboratory experiments on charge transfer

Most of the laboratory work in the 1970s and 1980s was performed by two groups; Saunders and colleagues at UMIST [3–5] and by Takahashi [6]. Their experiments usually involved rebounding collisions between ice particles of sizes ranging from tens of microns to millimeters, over a temperature range from close to 0 °C to −30 °C in the presence of water drops. The results are expressed in terms of sign and magnitude of charge transferred to the riming particle as a function of environmental temperature, EW, or 'effective liquid water content', [3,4], a measure of the liquid water actually participating in riming, drop size distribution, and in some cases other parameters. Fig. 1 shows the results produced by the two groups.

Additional experiments [7–10] using somewhat different setups have revealed further detailed parameter dependences of the collisional charging. Quantitative differences among these laboratory results have received extensive comment in the recent literature, largely because parameterizations of the results of the two groups in numerical models yield different thundercloud charging histories. (See, e.g., [11].) However, although the details of the resulting charge transfer varied somewhat from experiment to experiment, the basic character of the results shown in Fig. 1 has not been seriously changed. There is a range of temperatures and EW values for which collisions charge the riming target negatively. At higher temperatures and/or higher EW the rimer charges positively. At very low EW there may also be a regime in which the graupel charges positively, although this finding is in some dispute. High relative humidity in the cloud of impacting ice particles [10] increases positive charging of the rimer.

Further analysis of the charge transfer results shows:

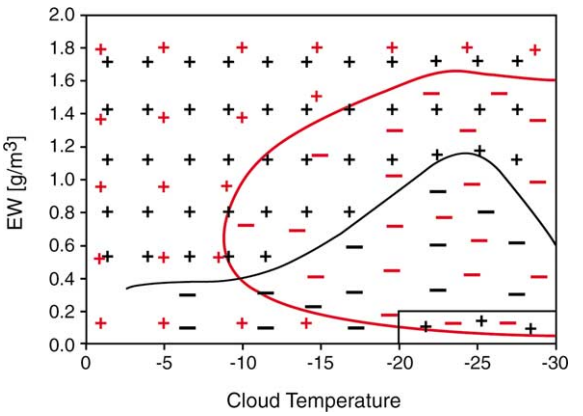

Figure 1. Sign of charge delivered to simulated rimer during laboratory tests of ice–ice collisional charging. EW: effective liquid water content (see text). Black: results from Saunders [3]. Red: results from Takahashi [6]. Negative charging of rimer was found by both groups at $T \leqslant -15$ °C, $0.4 \leqslant EW \leqslant 1.2$ g·m^{-3}, and both found positive charging of rimer at $T \geqslant -10$ °C, $EW \geqslant 0.4$ g·m^{-3}, but the results of the two laboratories differ in the rest of the parameter space tested. Adapted from figures kindly supplied by C.P.R. Saunders.

- the magnitude of the charge transferred generally increases with impact velocity and particle size;
- the sign of the charge varies with vapor growth rate; the most rapidly growing (or least rapidly sublimating) surface becomes positively charged by the collision;
- the magnitude of the negative charge to the graupel increases with the vapor growth rate of the small ice crystals;
- when the rimed ice surface is covered with frost (or water, at high temperatures) it charges positively in collisions with ice crystals.

Given the many approximations in the translation of laboratory experiments to the numerical models before the physical mechanism is well established, we focus mainly on the common features of the charging found in all the laboratory investigations.

1.2. Proposed charging mechanisms

A number of hypotheses have been put forward to attempt to explain these properties of collisional charging; of these, only a few detailed microphysical theories have been worked out, and these only for the (hypothetical) case of spatially infinite vapor grown crystals. Among the ideas that have been scrutinized are the thermoelectric effect [12], the Workman–Reynolds effect [13], exchange of surface melted layers formed on the ice particles prior to collision [14], surface tension anomalies [15], and creation of high concentrations of water ions at the ice surface by the growth itself [16,17].

A number of natural phenomena and laboratory experiments suggest that the ice/vapor interface is the locus of net electric charge, even in equilibrium. Measurements of dc and ac conductivities [18,19], surface potentials [18] and surface chemistry [20] all suggest that the surface layer contains greater net charge density than the bulk. It seems likely, therefore, that the charge transfer during ice–ice collisions involves the mixing and exchange of material from thin, charged, surface layers.

2. A new model of charge transfer in ice–ice collisions

2.1. Conceptual basis of the model

In the following paragraphs we summarize a new model of charge transfer during collisions involving a vapor grown ice crystal and a flatter, riming particle. The elements of this model are as follows:

- the formation of charged surface layers on each ice particle is due to electrostatic interactions among the charged species just inside the surface;
- we assume the effective charge carriers in ice are the water ions (H_3O^+, OH^-) and the Bjerrum defects, (L^-, D^+). Although the exact nature of the latter pair is now under debate, the traditional picture (that these are point defects characterized by mobilities and charges as are the water ions) is sufficient for our purposes. Note that the 'charge' on the Bjerrum defects is not free and cannot be transferred in collisions; rather it contributes to the internal electric field via polarization of the ice lattice, and the ions move in the resulting field. The polarization contribution cannot be neglected as the bulk concentrations of the Bjerrum defects in ice are approximately five orders of magnitude greater than those of the water ions [21];
- each of the four charge carriers obeys a conservation equation based on those first put forth by Jaccard [22]. Because we are particularly interested in the special region near the ice–vapor interface we supplement the Jaccard model with a description of the surface;
- the surface electric charge density is calculated from the concentrations of the four charge carriers as a function of the distance from the ice vapor interface and of the growth or sublimation rate;
- application of elasticity theory [23] to an approximate geometric model of the colliding surfaces, plus a collision parameterization that is fit to experiment, provide an estimate of the volume of ice that is melted in a collision;
- all the melted mass is assumed to be pushed from the sharper particle to the flatter one in the zone of contact;

- the charge that initially resided in the ice that melts is transferred with the melt fluid.

The temperature dependent charge transfer computed from the model is matched against laboratory observations of collisional charge transfer between flat rimed surfaces and ice crystals at equilibrium [24] and during vapor growth or sublimation [6,10].

We now describe this model in somewhat more detail.

2.2. The conservation equations

Following [22], each of the four charge carriers obeys a conservation equation that includes the following processes: (i) creation, (ii) annihilation, (iii) diffusion in the concentration gradient, (iv) drift in the electrostatic field created by the varying distributions of the four charged species. In a one-dimensional system, with x the (instantaneous) distance from the ice/vapor interface, our conservation equation for the concentration of the D^+ defect, for example, is

$$\frac{\partial c_D}{\partial t} = F_B - \frac{c_D c_L}{\overline{c_L}\tau_B} - \frac{\partial j_D}{\partial x}, \tag{1}$$

where F_B [$(m^3{\cdot}s)^{-1}$] is the creation rate for the Bjerrum defects, τ_B [s] the time scale for annihilation of D^+ and L^- defects, and the bulk average L^- concentration is $\overline{c_L}$. The current j_D [$(m^2{\cdot}s)^{-1}$] is given by

$$j_D = -D_D\frac{\partial c_D}{\partial x} - \mu_D q_D c_D E - v c_D, \tag{2}$$

where D_D, μ_D are the diffusion coefficient and the mobility of this defect, q_D its effective charge, E the electric field at x (found by solution of the Poisson equation, taking into account all four charged species) and v [$m{\cdot}s^{-1}$] is the growth or sublimation velocity. Eq. (2) shows that during sublimation or growth ($v \neq 0$), there is a current of defects relative to the interface even if they do not move from site to site.

Since the D^+ are much less mobile than the other ions [25] we assume here that $D_D = \mu_D = 0$, so that $j_D = -v c_D$.

2.3. Surface characterization

Surface disorder (for example, [26]) predicts that the activation energy for creation of defects and ions at the surface is lower than that in bulk, and therefore that the activation rates are anomalously high at the surface. Estimates [25] suggest that at equilibrium the ensuing Bjerrum defect and ionic concentrations are many orders of magnitude higher in a layer of several nanometers at the surface than in the bulk. These sharp gradients at the surface produce numerical instabilities in the solutions of the conservation equations (1) that preclude accurate predictions. We therefore solved the equations numerically for smaller surface gradients (defect creation rates up to about 100 times greater at the surface than in the bulk) and examined the results as we increased the surface anomalies. Robust trends in the solutions thus found allow simple interpretation of the charge rearrangement processes that do not depend on exact numerical calculations. In this paper we utilize the insights gained from this analysis to put forth a simpler model in which we avoid the numerical instabilities by prescribing surface defect concentration as a boundary condition on the solutions rather than calculating it. We show that the trends are consistent with those observed and that with reasonable values for the input parameters the quantitative results can be put in good agreement with measured charge transfers by adjustment of one free parameter. Further numerical investigation of the equations will be reported later.

2.4. Approximate solution of the conservation equations

Our findings to date strongly indicate that the least mobile defect (the D^+) dominates the electric field inside the ice surface both in equilibrium and during growth. OH^- are attracted to the surface and the L^+ and H_3O^+ repelled from the surface by the electric field produced by the surface excess D^+. The net effect is that the the surface is negatively charged and exhibits high dc and ac conductivity in both equilibrium and growth, consistent with measurements.

We write the concentration of the D^+ defects to first order in the growth velocity v as

$$c_{\mathrm{D}}(x) = c_{\mathrm{D,eq}}(x) + \delta_{\mathrm{D}}(x)v, \tag{3}$$

and the concentrations of the other species are of analogous form.

For the simple model to be discussed here, we calculate the growth contributions to these concentrations in terms of their equilibrium values and use ancillary laboratory data to set the (smaller) equilibrium surface concentrations.

The calculations show that the growth contribution to the surface concentration of D^+ is approximately that for which the rate of annihilation of D^+ with L^- equals the rate at which growth sweeps the D^+ inside the crystal. By expanding Eq. (1) to first order in the growth velocity, assuming that c_{L} is of the form shown in Eq. (3), and putting $\overline{c_{\mathrm{L}}} = c_{\mathrm{L,eq}}$, we find that in steady state

$$v\frac{\partial c_{\mathrm{D,eq}}(x)}{\partial x} = -\frac{v\delta_{\mathrm{D}}(x)}{\tau_{\mathrm{B}}}. \tag{4}$$

The charge that can be transferred from one particle to another resides on the surface ions and not on the defects. The growth rate contribution to the surface ion concentration is approximately that for which $\delta E_{\mathrm{I}}(0)$, the growth induced perturbation in surface electric field due to the ions, just cancels $\delta E_{\mathrm{B}}(0)$, the growth induced perturbation in the surface electric field due to the Bjerrum defects. That is,

$$\delta E_{\mathrm{I}} \sim q_{\mathrm{I}} \int_0^\infty (\delta_{\mathrm{H_3O^+}} - \delta_{\mathrm{OH^-}})\,\mathrm{d}x = -\delta E_{\mathrm{B}} = -q_{\mathrm{B}} \int_0^\infty (\delta_{\mathrm{D}} - \delta_{\mathrm{L}})\,\mathrm{d}x. \tag{5}$$

Here e is the electronic charge and $q_{\mathrm{I}} = 0.61e$, $q_{\mathrm{B}} = 0.38e$, the effective charges on the ions and on the Bjerrum defects [21]. Since the H_3O^+ are highly mobile, they retreat toward the crystal center and for the present we neglect their contribution to surface charging. In the approximation that the surface ionic field is dominated by the OH^- ions and the surface Bjerrum field by the D^+ defects, as suggested by our numerical results, we have

$$\delta\sigma \approx e \int \delta_{\mathrm{OH^-}}(x)\,\mathrm{d}x = -vq_{\mathrm{D}}\tau_{\mathrm{B}}c_{\mathrm{D,eq}}(0). \tag{6}$$

$\delta\sigma$ [C·m^{-2}] is the growth (or sublimation) induced perturbation in surface charge density. The measured electrical properties of the ice surface [27] are consistent with $c_{\mathrm{D,eq}}(0) \approx 3 \times 10^{27}$ [m^{-3}] at -10 °C. We assume this value is independent of temperature. We can estimate τ_{B} by calculating the time between arrivals of L^- defects, with bulk density $\overline{c_{\mathrm{L}}}$ and mobility μ_{L}, coming from the half space inside the crystal, at each stationary D^+ defect under the influence of the Coulombic attraction between the L^- and D^+ defects. This gives $\tau_{\mathrm{B}} \sim 6\varepsilon\varepsilon_0/(q_{\mathrm{L}}\mu_{\mathrm{L}}\overline{c_{\mathrm{L}}})$. The high frequency dielectric constant for ice is $\varepsilon = 3.16$, the effective charge $q_{\mathrm{L}} = -0.38e$ [21], and the average concentration $\overline{c_{\mathrm{L}}} = 3 \times 10^{21}$ [m^{-3}] at $T = -20$ °C with activation energy $E_{\mathrm{L}} = 0.73$ eV; $\mu_{\mathrm{L}} = 2 \times 10^{-8}$ [m^2·(V·s)$^{-1}$] at the same temperature with activation energy $E_\mu = 0.25$ eV [25], yielding $\tau_{\mathrm{B}} \approx 4.6 \times 10^{-5}$ [s] at -20 °C. With these parameters, and $v = 1$ μm·s^{-1} we find $\delta\sigma = -(2.4\times10^{-3}, 1.3\times10^{-2}, 8.6\times10^{-2})$ [C·m^{-2}] at $T = -10, -20, -30$ °C, respectively.

The equilibrium surface charge σ_{eq} can be inferred from measured equilibrium surface conductivities γ [25]. At

$$T = -10\ ^\circ\mathrm{C}, \qquad \gamma = 3 \times 10^{-11}\ [\mathrm{S}] = \sigma_{\mathrm{H_3O^+,eq}}\mu_{\mathrm{H_3O^+}} + |\sigma_{\mathrm{OH^-,eq}}|\mu_{\mathrm{OH^-}},$$

where $\sigma_{\mathrm{H_3O^+,eq}}$, $\sigma_{\mathrm{OH^-,eq}}$ [C·m^{-2}] are the equilibrium surface charge densities due to the ions. Since the H_3O^+ migrate toward the center of the crystal, $\sigma_{\mathrm{eq}} \approx \sigma_{\mathrm{OH^-,eq}} \gg \sigma_{\mathrm{H_3O^+,eq}}$. Assuming that $\mu_{\mathrm{OH^-}}$ near the surface is equal to its bulk value $\mu_{\mathrm{OH^-}} = 10^{-7}$ [m^2·(V·s)], which yields $\sigma_{\mathrm{eq}} \approx -3 \times 10^{-4}$ [C·m^{-2}]. The conductivity decreases with temperature as exp[-1.2 eV·kT^{-1}], leading to even smaller values of surface charge density at equilibrium at lower temperatures. The fact that $\delta\sigma > \sigma_{\mathrm{eq}}$ is consistent with

the observation that charge transfer between ice particles is larger during nonequilibrium than when the colliding particles are both in equilibrium.

The treatment presented here has been approximate since we have not solved the fully coupled conservation equations for all four species. However, we show below that this model as it stands gives semiquantitative agreement with the signs, magnitudes and temperature dependence of observed charge transfers.

2.5. Material exchange in collisions

Transfer of small amounts of mass has been observed during ice–ice collisions in association with transfer of electric charge [9]. Subsequent analysis [17] indicated the mass is probably melt. The direction of mass transfer must be determined by a physical difference between the two surfaces in contact. Experiments have demonstrated that the relevant difference is not simply that of temperature [18] or of surface ice density. Moreover, explanations based on difference in surface charge density alone [17] cannot explain measured charge transfers between two nongrowing ice particles [24]. One point that has been overlooked in previous treatments of charge transfer is the asymmetry in the radii of curvature between the colliding particles in realistic collisions, where it is likely that one sharp corner strikes a relatively flat surface.

We focus our attention here on collisions occurring below -10 °C, for which we can compare model predictions and data. In this temperature regime, the collision between a riming particle and an ice crystal generally charges the riming particle negatively. The ice crystal probably has the sharper corner because the rate of vapor growth of the rimed particle is likely to be significantly lower than that of the ice crystal [5]: the freezing-growth during riming tends to make relatively smooth surfaces whereas vapor growth produces flat facets with sharp corners. Imbedding of the sharper point [23], shearing off of the sharper point, or the flow of melt from the sharper point generally favors mass transfer to the flat surface.

We consider below the melting accompanying the collision of a small ice crystal of equivalent spherical radius R_{cr} with a flat ice surface. The relative velocity of the particles at impact is U [m·s^{-1}] and the tip of the ice crystal that contacts the flat surface is a spherical cap of initial radius of curvature r_{tip}. The maximum pressure at the contact area during elastic rebound is [28]

$$p_{\max}\ [\mathrm{MPa}] = 195(R_{\mathrm{cr}}/r_{\mathrm{tip}})^{0.6}U^{0.4}. \tag{7}$$

Pressure melting data [29] for temperatures $0 \geqslant T \geqslant -24$ °C can be well fit by the expression

$$p_{\mathrm{melt}}\ [\mathrm{MPa}](T) \approx -12.237T - 0.1171T^2. \tag{8}$$

By setting $p_{\mathrm{melt}} = p_{\max}$ we find $U_{\min}$, a minimum value for U for which collisions can produce pressure melting in the contact region. The results show that for $R_{\mathrm{cr}}/r_{\mathrm{tip}} = 1$, $U_{\min}$ ranges from a few centimeters/second at -5 °C to 1.6 meters/second at -25 °C, while for $R_{\mathrm{cr}}/r_{\mathrm{tip}} \geqslant 10$, $U_{\min} \ll 1$ m·s^{-1} for the entire temperature range. Since typical ice–graupel collision speeds in the laboratory charge transfer experiments and in thunderclouds are several to tens of meters per second, these results show that these collisions are very likely to produce pressure melting at the point of contact of the ice crystal and larger rimed particle. The melted mass can form on both particles but there will be a strong horizontal pressure gradient around the initially sharper particle that will force the melted material away from this particle and into the flatter one. We can estimate the volume of this mass by assuming the work done in pushing it aside is some fraction f of the loss of incident kinetic energy of the smaller particle; neglecting temperature changes in the region to the melting, viscous dissipation and refreezing, we have approximately that

$$V_{\mathrm{melt}} = \frac{fKE}{p_{\mathrm{melt}}} \tag{9}$$

$$= \frac{2\pi}{3}\frac{f\rho_i R_{\mathrm{cr}}^3 U^2}{p_{\mathrm{melt}}}. \tag{10}$$

The parameter f depends on the details of the collision. It is probably less than the inelasticity of the collision as measured by the momenta of the colliding particles before and after contact, because of complex mass and heat transfers at the point of contact. We will use f as a fit parameter in our discussion below.

Expression (10) is similar to the melt volume predicted in [17], but in that work they neglect the work needed to push the melt aside, so that their melted volume is larger than ours by a factor $\rho_l/(\rho_l - \rho_i) \approx 12$.

2.6. Charge transfer during collisions

A quantitative discussion of the collisional mass and charge transfer would have to depend on the geometry of the colliding surfaces and would involve details that cannot be known precisely. Therefore we analyze the charge transfer trends using the idealized geometry introduced above. We assume that in the temperature range of interest the collision melts a mass of volume V_{melt} in the spherical cap at the tip of a protruberance of the small ice crystal. (In other thermodynamic regimes the sharper protruberances will be found on the rimer; we discuss these other scenarios below.) This mass is assumed transferred from the initially sharper point to the flatter particle. The charge that is transferred with the melted mass is that on the surface of the initial spherical cap.

The surface area of such a cap of radius r_{tip} and bounding angle Θ_0 is

$$A(\Theta_0) = 2\pi r_{\text{tip}}^2(1 - \cos\Theta_0), \tag{11}$$

and the charge transferred in the collision is

$$\Delta Q = A(\Theta_0)\sigma_{\text{surface}}. \tag{12}$$

The surface area is related to the volume of material melted:

$$V_{\text{melt}} = V(\Theta_0) = \pi r_{\text{tip}}^3\big(2/3 - \cos\Theta_0 + \cos^3\Theta_0/3\big), \tag{13}$$

and for the realistic case that $\Theta_0 \leqslant 0.2$, we can approximate $A(\Theta_0) \approx 2\sqrt{\pi r_{\text{tip}} V(\Theta_0)}$. The surface charge density is

$$\sigma_{\text{surface}} = \sigma_{\text{eq}} + v\delta\sigma. \tag{14}$$

In the next section we use laboratory measurements for the special case of charge transfer between ice spheres and smooth ice surfaces at equilibrium to set f. We then use the best fit range of f to predict the charge transfer between real vapor grown ice particles as a function of growth/sublimation rates.

2.7. Charge transfer between frozen drops and ice surfaces in equilibrium

Laboratory experiments [24] showed that when ice spheres of radius $R_{\text{cr}} \leqslant 70$ [μm] near equilibrium collided with a large sublimating smooth ice surface at impact velocity U they lost an average amount of negative charge

$$\Delta Q_{\text{measured}}\ [\text{fC}] \approx -1.6 * U * (R_{\text{cr}}/50)^2, \tag{15}$$

at -10 °C. The charging predicted from Eq. (12) is

$$\Delta Q_{\text{model}}\ [\text{fC}] \approx 2\sqrt{\pi r_{\text{tip}} V_{\text{melt}}}\,\sigma_{\text{surface}}, \tag{16}$$

and, putting $R_{\text{cr}} = r_{\text{tip}}$, $\sigma_{\text{surface}} = \sigma_{\text{eq}}$ we have

$$\Delta Q_{\text{model}} \approx 2\sqrt{\frac{2\pi^2 f\rho_i R_{\text{cr}}^4 U^2}{3p_{\text{melt}}(T)}}\sigma_{\text{eq}} \tag{17}$$

$$= 2\sqrt{\frac{2\pi^2\rho_i}{3}}\sigma_{\text{eq}}\left[\frac{f}{p_{\text{melt}}(T)}\right]^{0.5} U R_{\text{cr}}^2. \tag{18}$$

Thus the model predicted dependence of the charging on R_{cr} and on U agree with the measurements.

We use the measured melting pressure (Eq. (8) in Eq. (18)) to match predicted ΔQ and the fit to the charge transfer observations (Eq. (15) at -10 °C. This requires that the product $\sigma_{eq} f^{0.5} = -4 \times 10^{-5}$ [C·m^{-2}] at this temperature, and we assume this product has the same value throughout the rest of our discussion. With the estimated equilibrium surface charge $\sigma_{eq} = -10^{-4}$ [C·m^{-2}] [25] this means $f = 0.16$.

In the next sections we will consider real vapor grown crystals, where the impacting crystal tip is much smaller than the effective spherical radius of the particle. Because the corners of the vapor-grown crystals are much sharper than the contact points from spherical crystals ($r_{tip} \approx 1-5$ μm at the contact points), the calculated charge transfers from the equilibrium charge at the surface are less than than those for the equilibrium spheres, all other parameters remaining constant. (See Eq. (16).)

2.8. Nonequilibrium charge transfer

We next estimate the amount of charge transfer in the case that the small particles are ice crystals growing from the vapor, again limiting ourselves to the temperature range below -10 °C. In this regime riming is due to drops of radii 15 μm and more that impact, flatten and freeze [30]. If part of the graupel surface is covered with frost, a facet region of an impinging ice crystal can rebound from sharp corners of the frost, thus leading to negative charge loss of the frost (equivalently, positive charge transfer to the graupel). Hence, in general, we expect large variations in ΔQ at high growth rates, as observed [24].

The total charge transferred is given by Eq. (12). Note that whereas previous models [31,17] were unable to explain positive charging of graupel when impacted by sublimating crystals, this follows directly from Eq. (14), since in the case of sublimation $v < 0$ and, as we have seen, for realistic growth or sublimation rates, $\delta\sigma$ is larger in magnitude than σ_{eq}.

2.9. Comparison to experiment

In order to compare with measured charge transfers we must relate R_{cr} to maximum crystal dimension D_{max}. Crystal growth experiments [32] show that for up to 5 minutes of vapor growth $R_{cr} \propto D_{max}^{1.7}$ for tabular crystals and $R_{cr}^3 \propto D_{max}^{1.03}$ for columnar crystals. Collision experiments [33] at -25 °C, $U = 10-50$ [m·s^{-1}] show that $\Delta Q \propto D^{0.6-0.8}$. For these parameters our model yields $\Delta Q \propto D^{0.5-0.9}$ (including columnar and tabular crystals). Thus the predicted trends match those observed quite well over this range. Results in conditions closer to typical thunderstorm conditions are shown in Fig. 2, which presents a range of model predicted values compared with average measured charge transfer [10] at the same temperatures, relative humidities and collision velocities, for two values of f (Eq. (10)) and of r_{tip}. Berdeklis and List [10] used drops of 20–30 μm diameter and most crystal sizes were between 50 and 100 μm in size. In this figure our predicted charge transfer results come from Eq. (12). Fig. 2 shows the measured trends with temperature are broadly similar to the calculations. Similar temperature trends were found by [5]. Note that the particularly large negative charge transfer we predict at -16 °C is consistent with results described in the text by [10]. The total calculated charge is typically within a factor of two of the measured charge. More accurate charge distribution profiles computed from the model that include the effects of the positive water ions further from the surface should decrease the dependence of charge transfer on impact velocity at high velocity, since at high impact velocity so much ice melts that part of the melted mass contains significant positive charge as well as negative.

The predicted peaks in the charging near -14.4 °C are due to the peaks in v and in R_{cr} at this temperature, and they match observations. Thus the variation in vapor growth rate dominates the temperature trend of the magnitude of the charge transfer, a fact that has not been explicitly noted in previous model studies. This relationship explains the oft-stated hypothesis [4,5] that "the particle that is growing fastest from the vapor (or sublimating slowest) charges positively".

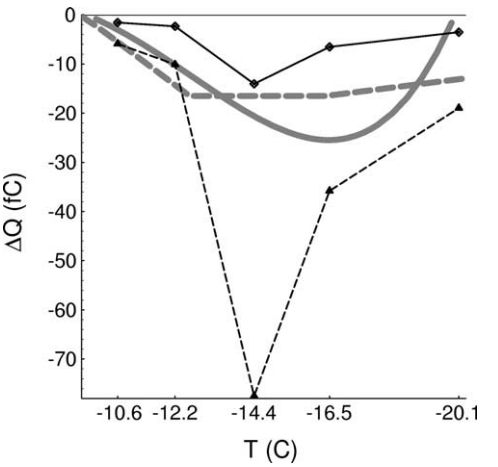

Figure 2. Charge transfer per collision to riming particle. Thick dashed line: experimental data derived from results of [6] at cloud liquid water content of 1.1 [g·m^{-3}]. Thick solid line; maximum measured charge transfers near water saturation, $EL = 0.5$ [g·m^{-3}] [10]. Thin solid line: calculations for $r_{\text{tip}} = 2$ µm, $f = 0.03$. Thin dashed line: calculations for $r_{\text{tip}} = 8$ µm, $f = 0.3$. All calculations assumed $U = 5.3$ m·s^{-1}, using measured crystal masses and growth rates (after 3 minutes of growth) from [32].

3. Discussion

Although our detailed numerical simulations of realistic internal charge carrier concentrations have not been fully completed, extraction of the major physical features of preliminary numerical calculations has allowed us to present a semiquantitative model with only one adjustable parameter. The estimated charge transfer based on the new model appears broadly consistent with data both at equilibrium and in the situation in which vapor growth effects have been included.

We have applied the model to collisions between dry surfaces at temperatures $T \leqslant -10$ °C, where the graupel surface is fairly flat and receives negative charge during collisions with vapor grown crystals. We can speculate as to the extension of this model to other thermodynamic regimes.

At higher temperatures and/or high effective liquid water contents the graupel surface may be so soft that most crystals will be captured and a rebounding crystal may scoop up surface material and carry it off. Thus in this regime we expect the graupel surface to charge positively as a result of rebounding collisions in this regime.

At low effective liquid water contents and moderately high temperatures the graupel surface may contain patches of frost. The frost points may be sharper than those on the ice crystals and thus may become imbedded in the ice crystals, or they can even fracture on contact [6,8]. Either of these would produce the sometimes observed positive charging of graupel at low ambient liquid water content.

According to our model, charge travels from particle to particle via mass transfer. The inductive theory of ice–ice charging, on the other hand, was based on the hypothesis that induced charge transfers via conduction, which is a slower process, leading to the conclusion that the inductive mechanism is not effective in the early stages of thunderstorm evolution. This conclusion should be revisited in the light of our new model; it may be more effective than now thought. The new model may also explain the large observed charge transfers during ice–ice induction experiments [34], which the conduction mechanism cannot explain.

Our results are sensitive to the factor f, defining the fraction of incoming energy that goes to pressure melting, and to the assumed shape of the colliding surfaces. The surface of a rimed particle during growth contains smooth regions from just-frozen droplets, still liquid unfrozen droplet and frost from vapor growth, particularly near the droplets. The distributions and properties of these regions near collision sites has not been determined. The effects of local structure on the amount of melt in a collision and on the amount of surface charging before the collision can be significant and variable. Furthermore, ice at relevant temperatures has complex mechanical properties, rendering difficult, if not impossible, the task of quantitatively describing the mechanics of the collisions. Moreover, laboratory studies on effects of

impurities [4] and even of different cloud mixing regimes on ultimate charging show that it will always be difficult to extrapolate the results of laboratory experiments to the atmosphere.

However, the new model appears to have a solid physical foundation, it matches observed trends and is consistent with data from a wide range of sources. It constitutes an important step in understanding the electrical properties of the ice vapor surface and thunderstorm electrification.

Acknowledgements. J. Nelson thanks Gakushin University for support through a JSPS fellowship. We thank the Bosack–Kruger Foundation for partial support of this research.

References

[1] J. Latham, The electrification of thunderstorms, Q. J. Roy. Met. Soc. 107 (1961) 277–298.
[2] A.J. Illingworth, Charge separation in thunderstorms: small scale processes, J. Geophys. Res. 90 (1985) 6026–6032.
[3] C.P.R. Saunders, Thunderstorm electrification experiments and charging mechanisms, J. Geophys. Res. 99 (1994) 10773–10779.
[4] E.R. Jayaratne, C.P.R. Saunders, J. Hallett, Laboratory studies of the charging of soft-hail during ice crystal interaction, Q. J. Roy. Met. Soc. 109 (1983) 609–630.
[5] B. Baker, et al., The influence of diffusional growth rates on the charge tranfer accompanying rebounding collisions between ice crystals and hailstones, Q. J. Roy. Met. Soc. 113 (1987) 1193–1215.
[6] T. Takahashi, Riming electrification as a charge generation mechanism in thunderstorms, J. Atmos. Sci. 35 (1978) 1536–1548.
[7] J.P. Rydock, E. Williams, Charge separation associated with frost growth, Q. J. Roy. Met. Soc. 117 (1991) 409–420.
[8] E.E. Avila, et al., Charging in ice–ice collisions as a function of the ambient temperature and the larger particle average temperature, J. Geophys. Res. 101 (1996) 29609–29614.
[9] B. Mason, J.G. Dash, Charge and mass transfer in ice–ice collisions: experimental observations of a mechanism in thunderstorm electrification, J. Geophys. Res. 105 (2000) 10185–10192.
[10] P. Berdeklis, R. List, The ice crystal–graupel collision charging mechanism of thunderstorm electrification, J. Atmos. Sci. 58 (2001) 2751–2770.
[11] J. Helsdon, et al., An examination of thunderstorm charging mechanisms using a two-dimensional storm electrification model, J. Geophys. Res. 106 (D1) (2001) 1165–1192.
[12] J. Latham, B.J. Mason, Electric charge transfer associated with temperature gradients in ice, Proc. Roy. Soc. A 260 (1961) 523–536.
[13] E.J. Workman, S.E. Reynolds, Electric phenomena occurring during the freezing of dilute aqueous solutions and their possible relationship to thunderstorm electricity, Phys. Rev. 78 (1950) 254–259.
[14] M.B. Baker, J.G. Dash, Mechanism of charge transfer between colliding ice particles in thunderstorms, J. Geophys. Res. 99 (1994) 10621–10626.
[15] A. Graciaa, P. Creux, J. Lachaise, R. Schechter, Charge transfer between colliding hydrometeors: role of surface tension gradients, J. Geophys. Res. 106 (D8) (2001) 7967–7972.
[16] T. Takahashi, Electric surface potential of growing ice crystals, J. Atmos. Sci. 27 (1970) 453–562.
[17] J.G. Dash, B.L. Mason, J.S. Wettlaufer, Theory of charge and mass transfer in ice–ice collisions, J. Geophys. Res. 106 (2001) 20395–20402.
[18] J.M. Caranti, A.J. Illingworth, Frequency dependence of the surface conductivity of ice, J. Phys. Chem. 87 (1983) 4078–4083.
[19] N. Maeno, Measurements of surface and volume conductivities of single ice crystals, in: E. Whalley, et al. (Eds.), Physics and Chemistry of Ice, Royal Society of Canada, Ottawa, 1973, pp. 140–143.
[20] T. Huthwelker, D. Lamb, M.B. Baker, B.D. Swanson, Th. Peter, Uptake of SO_2 by polycrystalline water ice, J. Coll. Interf. Sci. 238 (2001) 147–159.
[21] P.V. Hobbs, Ice Physics, Academic Press, 1974.
[22] C. Jaccard, Thermoelectric effects in ice crystals I. Theory of the steady state, Phys. Kondens. Materie 1 (1964) 143–151.
[23] L. Landau, E.M. Lifshitz, Theory of Elasticity, Vol. 7, Course of Theoretical Physics, Pergamon Press, 1959, Section 9, Problem 1.
[24] W. Gaskell, A.J. Illingworth, Charge transfer accompanying individual collisions between ice particles and its role in thunderstorm electrification, Q. J. Roy. Met. Soc. 106 (1980) 841–854.
[25] V.F. Petrenko, R.W. Whitworth, Physics of Ice, Oxford University Press, Oxford, 1999.
[26] N. Fletcher, Surface structure of water and ice. II. A revised model, Phil. Mag. 18 (1968) 1287–1300.

To cite this article: M. Baker, J. Nelson, C. R. Physique 3 (2002) 1293–1303

[27] V.F. Petrenko, I.A. Ryzhkin, Surface states of charge carriers and electrical properties of the surface layer of ice, J. Phys. Chem. B 101 (1997) 6285–6289.
[28] M. Higa, M. Arakawa, N. Maeno, Size dependence of restitution coefficients of ice in relation to collision strength, Icarus 133 (1998) 310–320.
[29] Y. Kishimoto, M. Maruyama, Growth of ice I_h in water and measurements of its melting curve, Rev. High Pressure Sci. Technol. 7 (1998) 1144–1146.
[30] H.R. Pruppacher, J.D. Klett, Microphysics of Clouds and Precipitation, 2nd edition, Kluwer Academic, Norwell, MA, 1997.
[31] C.R. Saunders, S.L. Peck, G.G. Aguirre Varela, E.E. Avila, N.E. Castellano, A laboratory study of the influence of water vapour and mixing on the charge transfer process during collisions between ice crystals and graupel, Atmos. Res. 58 (2001) 187–203.
[32] T. Takahashi, et al., Vapor diffusional growth of free-falling snow crystals between -3 and -23 °C, J. Met. Soc. Japan 69 (1991) 15–30.
[33] W.D. Keith, C.P.R. Saunders, Charging of aircraft: high-velocity collisions, J. Aircraft 27 (1990) 218–222.
[34] W.D. Scott, Z. Levin, The effect of potential gradients on the charge separation during interactions of snow crystals with an ice sphere, J. Atmos. Sci. 27 (1970) 463–473.